Phytopathology® • 2020 • 110:1845-1853 • https://doi.org/10.1094/PHYTO-04-20-0130-R

Population Biology

e-Xtra*

One Clonal Lineage of *Calonectria pseudonaviculata* Is Primarily Responsible for the Boxwood Blight Epidemic in the United States

Vanina L. Castroagudín,[1,2] Jerry E. Weiland,[3] Fulya Baysal-Gurel,[4] Marc A. Cubeta,[5] Margery L. Daughtrey,[6] Nicole Ward Gauthier,[7] James LaMondia,[8] Douglas G. Luster,[9] Francesca Peduto Hand,[10] Nina Shishkoff,[9] Jean Williams-Woodward,[11] Xiao Yang,[2,9] Nicholas LeBlanc,[1,2,5] and Jo Anne Crouch[1,†]

[1] U.S. Department of Agriculture-Agricultural Research Service, Mycology and Nematology Genetic Diversity and Biology Laboratory, Beltsville, MD 20705
[2] Oak Ridge Institute for Science and Education, ARS Research Participation Program, Oak Ridge, TN 37830
[3] U.S. Department of Agriculture-Agricultural Research Service, Horticultural Crops Research Laboratory, Corvallis, OR 97339
[4] Department of Agricultural and Environmental Sciences, Otis L. Floyd Nursery Research Center, Tennessee State University, McMinnville, TN 37110
[5] Center for Integrated Fungal Research, Department of Entomology and Plant Pathology, North Carolina State University, Raleigh, NC 27606
[6] School of Integrative Plant Science, College of Agriculture and Life Sciences, Cornell University, Ithaca, NY 14853
[7] Department of Plant Pathology, University of Kentucky, Lexington, KY 40546
[8] Connecticut Agricultural Experiment Station, Valley Laboratory, Windsor, CT 06095
[9] U.S. Department of Agriculture-Agricultural Research Service, Foreign Disease-Weed Science Research Unit, Frederick, MD 21702
[10] Department of Plant Pathology, The Ohio State University, Columbus, OH 43210
[11] Department of Plant Pathology, University of Georgia, Athens, GA 30602
Accepted for publication 23 June 2020.

ABSTRACT

Boxwood blight caused by *Calonectria pseudonaviculata* and *C. henricotiae* is destroying cultivated and native boxwood worldwide, with profound negative economic impacts on the horticulture industry. First documented in the United States in 2011, the disease has now occurred in 30 states. Previous research showed that global *C. pseudonaviculata* populations prior to 2014 had a clonal structure, and only the *MAT1-2* idiomorph was observed. In this study, we examined *C. pseudonaviculata* genetic diversity and population structure in the United States after 2014, following the expansion of the disease across the country over the past 5 years. Two hundred eighteen isolates from 21 states were genotyped by sequencing 11 simple sequence repeat (SSR) loci and by *MAT1* idiomorph typing. All isolates presented *C. pseudonaviculata*-specific alleles, indicating that *C. henricotiae* is still absent in the U.S. states sampled. The presence of only the *MAT1-2* idiomorph and gametic linkage disequilibrium suggests the prevalence of asexual reproduction. The contemporary *C. pseudonaviculata* population is characterized by a clonal structure and composed of 13 multilocus genotypes (SSR-MLGs) unevenly distributed across the United States. These SSR-MLGs grouped into two clonal lineages (CLs). The predominant lineage CL2 (93% of isolates) is the primary contributor to U.S. disease expansion. The contemporary U.S. *C. pseudonaviculata* population is not geographically subdivided and not genetically differentiated from the U.S. population prior to 2014, but is significantly differentiated from the main European population, which is largely composed of CL1. Our findings provide insights into the boxwood blight epidemic that are critical for disease management and breeding of resistant boxwood cultivars.

Keywords: *Buxus*, emerging disease, population biology, population structure, woody ornamentals

Boxwood blight disease is a major threat to the ornamental horticulture industry in the United States and worldwide (LeBlanc et al. 2018), and to native populations of boxwood (*Buxus* spp., *Buxaceae*) in Europe and southwest Asia (Decocq et al. 2014; Mitchell et al. 2018). The disease also affects two other genera in the family *Buxaceae*: *Pachysandra* (pachysandra) and *Sarcococca* (sweetbox), commonly grown as companion plants near boxwood in cultivated landscapes (Kong et al. 2017a, b; LaMondia et al. 2012; Malapi-Wight et al. 2016; Ryan et al. 2018). The financial loss in the horticultural sector due to boxwood blight is sizable, with the majority of economic damage and impact occurring in the nursery industry due to plant death, or the need to increase fungicide use to manage the disease (Daughtrey 2019).

Boxwood blight is caused by two sister species of invasive ascomycete fungi in the family Nectriaceae, namely *Calonectria pseudonaviculata* (syn. = *Cylindrocladium pseudonaviculatum* and *Cylindrocladium buxicola*) and *Calonectria henricotiae* (Gehesquière et al. 2016). The two species are distinguished from each other based on the application of genealogical concordance species recognition criteria, with a species divergence time estimated at 2.1 million years ago (Gehesquière et al. 2016; Malapi-Wight et al. 2019). *C. pseudonaviculata* and *C. henricotiae* share identical sequences of the internal transcribed spacer (ITS) region, but can be distinguished by fixed single nucleotide polymorphisms (SNPs) in the beta-tubulin (two SNPs), calmodulin (two SNPs), and histone H3 (two SNPs) loci (Gehesquière et al. 2016). One study also showed intraspecific

†Corresponding author: J. A. Crouch; joanne.crouch@usda.gov

Current address of N. LeBlanc: USDA-ARS, Crop Improvement and Protection Research Unit, Salinas, CA 93905.

Funding: Funding was provided by the USDA-ARS projects 2072-22000-043-00-D and 8042-22000-298-00-D, USDA-ARS Floriculture Nursery Research Initiative project (0500-00059-001-00-D), the USDA-APHIS Farm Bill 10007 program, and by the appointments of V. L. Castroagudín and X. Yang through an interagency agreement between the U.S. Department of Energy (DOE) and the USDA. ORISE is managed by ORAU under DOE contract number DE579AC05-06OR23100.

Mention of trade names or commercial products in this publication is solely for the purpose of providing specific information and does not imply recommendation or endorsement by the USDA. USDA is an equal opportunity provider and employer.

*The *e*-Xtra logo stands for "electronic extra" and indicates that supplementary tables and three supplementary figures are published online.

The author(s) declare no conflict of interest.

length and sequence polymorphisms in 39% of 1,359 simple sequence repeat (SSR) loci examined (LeBlanc et al. 2019). In addition, *C. pseudonaviculata* and *C. henricotiae* have different idiomorphs at the *MAT1* mating-type locus (Malapi-Wight et al. 2019). All known isolates of *C. henricotiae* contain the *MAT1-1* idiomorph, while all known isolates of *C. pseudonaviculata* have the *MAT1-2* idiomorph (Gehesquière et al. 2016; Malapi-Wight et al. 2019). In both cases, the mating loci show a gene arrangement consistent with those reported for heterothallic fungi in the Ascomycota and no intraspecific nucleotide variation among isolates of the same species (Malapi-Wight et al. 2019). Interestingly, despite both species being heterothallic, with complementary mating types (Malapi-Wight et al. 2019) and a sympatric geographic distribution (LeBlanc et al. 2019), neither hybridization or successful mating between *C. pseudonaviculata* and *C. henricotiae* has been observed in nature or successfully achieved in laboratory experiments (Gehesquière et al. 2016; LeBlanc et al. 2019; Malapi-Wight et al. 2019).

Phenotypic differences between the two species are also scarce (Gehesquière et al. 2016). In general, *C. pseudonaviculata* and *C. henricotiae* are not distinguishable by macroscopic or microscopic morphological characters (Gehesquière et al. 2016). Cultures of *C. henricotiae* often have smaller microsclerotia (N. Shishkoff, *personal communication*, data not shown) but this difference is not seen for microsclerotia produced in leaf tissue (Shishkoff, 2016). Virulence differences between the two species (i.e., host range, aggressiveness, or lesion morphology) have not been reported (Gehesquière et al. 2016). However, isolates of *C. henricotiae* are shown to be more thermotolerant than isolates of *C. pseudonaviculata*, as indicated by higher growth rates and higher levels of sporulation of *C. henricotiae* during in vitro tests (Gehesquière et al. 2016; Miller et al. 2018). In addition, *C. henricotiae* isolates are shown to be less sensitive than *C. pseudonaviculata* isolates to sanitizers and to certain fungicide classes (demethylation inhibitors [DMI] and quinone outside inhibitors [QoI]) (Gehesquière et al. 2016; Shishkoff 2016). The lower sensitivity of *C. henricotiae* to DMI chemistries has recently been correlated with presence of an intact *CYP51A* gene in *C. henricotiae* instead of the nonfunctional truncated *CYP51A* paralog found in *C. pseudonaviculata* (Stravoravdis et al. 2020).

The boxwood blight pathogens are hypothesized to have been introduced to Europe and subsequently to western Asia and North America via the commercial trade of boxwood plants from East Asia (Daughtrey 2019; LeBlanc et al. 2019). Boxwood plants with blight symptoms were first discovered in nurseries in the United Kingdom in 1994, and in New Zealand in 1998 (Crous et al. 2002; Henricot et al. 2000). In continental Europe, boxwood blight was first reported in Belgium in 2003, and since then the disease has spread across the entire continent (LeBlanc et al. 2018). In Asia, boxwood blight was first documented in the early 2010s when the disease began seriously affecting native stands of boxwood in the Eastern Black Sea region (Mitchell et al. 2018). The disease is now present across the Caucasus forests in Abkhazia, Iran, Georgia, and Turkey (Khazaeli et al. 2018; Mitchell et al. 2018). Boxwood blight was first detected in Canada in British Columbia in 2011 (Elmhirst et al. 2013). During that same year, the disease was reported for the first time from the United States in North Carolina, Connecticut, and Oregon (Ivors et al. 2012; Sacher et al. 2020). To date, boxwood blight is present in 30 states in the United States (Castroagudín et al. 2020).

Population genetics is an invaluable tool to understand the evolutionary processes involved in pathogen invasions and migrations, emergence of new diseases, and evolution of host–pathogen interactions (Milgroom 2017). Information on population genetic diversity and structure of the boxwood pathogens *C. pseudonaviculata* and *C. henricotiae* is still relatively limited (Khazaeli et al. 2018; LeBlanc et al. 2019). After the first global outbreaks of boxwood blight, Henricot and Culham (2002) used amplified fragment length polymorphism (AFLP)-based genetic markers to show that 15 *C. pseudonaviculata* isolates from the two earliest known outbreak locales in the United Kingdom and New Zealand shared the same AFLP profiles. Phylogenetic analyses used to screen a small number of samples of *C. pseudonaviculata* and *C. henricotiae* isolates also found no intraspecific genetic diversity (Crous et al. 2002; Gehesquière et al. 2016; Henricot and Culham 2002; Khazaeli et al. 2018). In the most comprehensive study published to date, LeBlanc et al. (2019) examined a global collection of 306 *Calonectria* isolates (*C. pseudonaviculata* n = 270; *C. henricotiae* n = 36) sampled between 1994 and 2014 from four continents and 16 countries, including 54 *C. pseudonaviculata* isolates recovered from nine states during the initial U.S. expansion of the disease from 2011 to 2014 (LeBlanc et al. 2019). In that study, *Calonectria* isolates were genotyped with 11 SSR loci shown to be polymorphic between and within *C. pseudonaviculata* and *C. henricotiae*. The results of LeBlanc et al. (2019) showed that *C. henricotiae* isolates were present in five European countries (Belgium, Germany, Slovenia, The Netherlands, and the United Kingdom) and that all isolates of *C. henricotiae* (except one) were genetically uniform across the SSR loci (LeBlanc et al. 2019). In contrast, *C. pseudonaviculata* was present worldwide, with 14 multilocus genotypes (SSR-MLG G1 to SSR-MLG G14). Two SSR MLGs, SSR-MLG G1 and SSR-MLG G2, were sampled in the highest frequency and represented 47 and 26% of the samples, respectively. SSR-MLG G1 was isolated from infected boxwood plants on four continents and it included the initial boxwood samples recovered from the United Kingdom and New Zealand in the 1990s. SSR-MLG G2 was found in Europe and North America; SSR-MLG G3 was recovered from Asia and Europe; and SSR-MLG G4 was found exclusively in Asia. The remaining genotypes (SSR-MGR G5 to SSR-MLG G14) were only found in European samples. All *C. pseudonaviculata* populations worldwide, including the U.S. *C. pseudonaviculata* population, showed low levels of gene and genotypic diversity, predominance of one mating type (*MAT1-2*) and linkage disequilibrium, characteristics consistent with invasive, clonal fungal plant pathogens (LeBlanc et al. 2019; Malapi-Wight et al. 2019).

LeBlanc et al. (2019) examined samples from a few major outbreak sites from nine states in the United States and during the initial 3 years of the boxwood blight epidemic in the United States. However, a comprehensive investigation of the genetic diversity and structure of the contemporary *C. pseudonaviculata* population associated with increased disease spread, particularly throughout the Pacific Northwest, Northeast, and mid-Atlantic regions has not been conducted (Daughtrey 2019; LeBlanc et al. 2018). Therefore, we set out to answer the following questions. (i) Is the contemporary U.S. population of *C. pseudonaviculata* different from the genotypes present during the initial introduction and expansion of the disease in Europe and the United States? (ii) Are there new genotypes present in the expanded geographical range of the U.S. epidemic? (iii) What is the contribution of sexual reproduction in *C. pseudonaviculata* populations to the boxwood blight epidemic? (iv) Are there genetic differences among the *C. pseudonaviculata* isolates infecting boxwood, pachysandra, and sweetbox? To address these questions, we examined 218 new isolates of *C. pseudonaviculata* recovered from 21 states in the United States between 2014 to 2019, and genotyped them with 11 SSR markers using a next-generation sequencing approach.

MATERIALS AND METHODS

Sample collection, isolation, and DNA extraction. A total of 218 isolates of *Calonectria* from plants exhibiting boxwood blight symptoms in 21 states in the United States were collected. From this total, 214 were obtained from *Buxus* spp., two from *Sarcococca hookeriana*, and two from *Pachysandra terminalis*

(Table 1, Supplementary Table S1). The majority of diseased plant material was obtained from diagnostic laboratories and other sources as disease outbreaks were identified between 2014 and 2019. In addition, to determine the extent of the disease in Oregon nursery production, during 2019 we conducted a stratified sampling in seven nurseries throughout the Willamette Valley. We sampled 5 to 10 blocks of stock plants per nursery, and collected 2 to 10 infected boxwood samples per block.

Fungal isolations from diseased plant material were conducted as described (Salgado-Salazar et al. 2019), and all cultures were purified by hyphal tip transfer under a Zeiss V20 stereoscope (Carl Zeiss Microscopy, Thornwood, NY). To produce material for DNA extraction, isolates were cultured on potato dextrose agar (PDA; Fisher Scientific, Pittsburg, PA) amended with streptomycin and neomycin (0.3 g/liter, Sigma-Aldrich, St. Louis, MO). Plates were incubated at 25°C under continuous fluorescent light for 7 days. Actively growing mycelia were harvested by adding 2 ml of sterile, deionized water to the PDA plate and scraping the plate surface with a sterile spatula. Harvested mycelia were transferred to a 75-ml-Erlenmeyer flask containing clarified V8 juice media (V8 vegetable juice; Campbells, Camden, NJ) prepared as described by Tuite (1969) without addition of $CaCO_3$. Liquid cultures were incubated at 24 to 26°C for 7 days under continuous fluorescent light and constant shaking (100 rpm). Mycelia were collected by vacuum filtration and stored at –80°C until use. Fungal tissue was frozen in liquid nitrogen and ground to a fine powder with mortar and pestle. Genomic DNA was extracted from the homogenate using the OmniPrep kit (G-Biosciences, St. Louis, MO). DNA quality and quantity were assessed through 1% agarose gel electrophoresis and using the Qubit 2.0 fluorometer (Invitrogen, Carlsbad, CA), respectively.

SSR genotyping-by-sequencing (GBS). *C. pseudonaviculata* isolates were genotyped with 11 SSR markers (Table 2, Supplementary Table S2) as previously described by LeBlanc et al. (2019) with modifications for implementation for GBS using Illumina technology (Beirn et al. 2017). In this study, we used the GBS approach because it provides both fragment length and sequence information for the loci of interest and avoids misinterpretation that could arise due to size homoplasy that would remain undetected by length assessment methods alone (Šarhanová et al. 2018; Tibihika et al. 2018). Illumina sequence reads do have an error rate of two to three magnitudes higher than reads generated through Sanger sequencing technology (10^{-3} versus 10^{-4} to 10^{-5}, respectively) (Fox et al. 2014; Ma et al. 2019). However, computational procedures such as those used in our study (described below), which subjected the raw reads to amplicon error correction, noise and chimera removal, and filtering of reads with low quality scores, have been shown to suppress next generation sequencing error rates to 10^{-5} to 10^{-4}, which is comparable to the average rate estimated for Sanger technologies (Ma et al. 2019). Additionally, Sanger reads are typically generated only at a coverage of 2×; in contrast, Illumina reads are typically generated to produce millions of reads from one starting DNA template molecule, resulting in a much higher depth of coverage. In the current study, we recorded an average coverage of 3,500× in the SSR repeated motif regions of interest.

For Illumina sequencing, SSR-specific primers were extended by adding Illumina Nextera adapters at the 5′ end of the forward and reverse primers, respectively, as described by LeBlanc and Crouch (2019). Post-amplification amplicons were pooled, purified using the Genomic DNA Clean and Concentrator kit (Zymo Research, Irvine, CA) and indexed with Nextera XT Index kit v.2 (Illumina, Inc., San Diego, CA) to produce amplicon libraries for sequencing. Libraries were pooled in batches of 94 isolates, purified as described above, and quantified using the KAPA Library Quantification kit (LightCycler 480 qPCR Mix; Roche Life Science, Madison, WI). After normalization, libraries were sequenced on a MiSeq sequencer (Illumina) using a paired-read 600-cycles cartridge and MiSeq Reagent kit v.3 (Illumina). PCR amplification and sequencing reactions that yielded new alleles were repeated twice (for a total of three independent repeats). Isolates CB002 (*C. pseudonaviculata*, genotype SSR-MLG G1; in-house ID JAC14-13) and NL018 (*C. henricotiae*, genotype SSR-MLG H1; in-house ID JAC14-101) previously characterized by LeBlanc et al. (2019) were included in each 96-sample set as positive and across-sequencing-run controls.

Sequence reads were quality checked and trimmed for removal of adapters and low-quality regions (Phred < 30) using Geneious Prime 20.0.4 (Biomatters Inc, San Diego, CA). Pairs of reads were merged using PEAR version 0.9.4 (Zhang et al. 2014) considering only minimum overlaps of 15 bp with a $P < 0.01$ for the highest observed expected alignment scores. The resulting assemblies were used for SSR allele calling using the software pipeline (scripts 1, 2, and 3) designed by Tibihika et al. (2018). The number of repeats and sequence sizes representing each allele of the SSR loci examined are detailed in Table 3.

TABLE 2. Simple sequence repeat (SSR) markers used to genotype isolates of *Calonectria pseudonaviculata*

SSR locus[a]	Repetitive motif	Number of alleles	Observed alleles[b]	
			Size (bp)	Number of repeats
368	CAA	3	495, 498, 501	17, 18, 19
610	AAC	2	481, 484	19, 20
662	AC	2	319, 321	17, 18
1281	CAGCA	2	330, 335	14, 15
1455	AC	1	325	13
1647	ACA	2	278, 281	14, 15
1816	GAA	1	316	17
2134	GAGCAT	2	357, 363	13, 14
2373	TTCA	2	367, 371	12, 13
2683	CTGCT	2	396, 406	10, 12
4152	CA	1	370	13

[a] SSR markers previously described by LeBlanc et al. (2019).
[b] Observed allele size includes repetitive motif, flanking region, and primers without Illumina adapters.

TABLE 1. Populations of *Calonectria pseudonaviculata* from the United States examined in this study

Population[a]	Sample origin			n[b]
	Year	State	Host	
East2014	2014, 2015, 2016	CT, DE, MD, NJ, NY, NC, PA	*Buxus* spp., *Sarcococca hookeriana*	35
East2017	2017	GA, IL, NC, NY	*Buxus* spp.	22
East2018	2018	CT, IN, KY, MD, MI, NC, NJ, NY, PA, SC, TN, WI	*Buxus* spp., *S. hookeriana*	48
East2019	2019	AR, GA, NC, NY, OH, TN	*Buxus* spp., *Pachysandra terminalis*	37
West2017	2017, 2018	CA, OR, WA	*Buxus* spp.	7
West2019	2019	OR	*Buxus* spp.	69
Total				218

[a] Isolates were assigned a priori into six populations determined by sampling year and geographic origin of the samples.
[b] n, total number of isolates.

Sequence data were examined to detect homoplasy (SNPs) in the SSR loci among isolates sharing the same SSR genotype. Paired end reads were mapped to reference sequences (Table 2) retrieved from the National Center of Biotechnology Information GenBank. Assemblies were then scanned with the *Find variations/SNPs* tool in Geneious Prime v. 2020.0.4 (Biomatters Inc., San Diego, CA) using default options and the minimum variant frequency set to 0.80. A multilocus SSR genotype (SSR-MLG) was assigned to each isolate using GENODIVE v. 3.03 (Meirmans and Van Tienderen 2004). Isolates exhibiting the same SSR-MLG were considered clones. Genotypes were named following the denomination adopted by LeBlanc et al. (2019). New SSR-MLGs were assigned with an identifier number from 15 to 24, in order of discovery.

Determination of mating-type idiomorphs. Idiomorph identity at the mating-type locus *MAT1* was determined using the PCR assay developed by Malapi-Wight et al. (2019). In this test, idiomorphs are identified by size polymorphisms in PCR products, with *MAT1-1* primers amplifying a fragment of 583 bp, and *MAT1-2* primers amplifying a fragment of 452 bp. The isolates CB002 (*C. pseudonaviculata*, *MAT1-2*) and NL018 (*C. henricotiae*, *MAT1-1*) previously characterized by LeBlanc et al. (2019) were used as positive controls. Sterile deionized water was used as a negative control in PCR reactions.

Characterization of contemporary *C. pseudonaviculata* populations. In this study we operationally define a population as a group of individuals of the same species that occupy the same general area at the same time, with a common evolutionary history (Milgroom 2017). For initial characterization, the 218 *C. pseudonaviculata* isolates were divided a priori into six populations according to the year of sampling (2014, 2017, 2018, and 2019) and geographical origin (West or East region of the United States) (Table 1). The six populations determined a priori were defined: East2014, East2017, East2018, East2019, West2017, and West2019 (Table 1). Summary statistics describing gene and genotypic diversity, richness, clonal fraction, and evenness (Table 4) were calculated with the *Poppr* package (Kamvar et al. 2014) in the R environment (R Core Team 2016). Except for the analysis of genotypic diversity, all following analyses used clone-corrected datasets in which only one individual from each multilocus microsatellite genotype was included per population.

A minimum spanning network (MSN) was constructed to analyze and visualize the distribution and genetic similarity among SSR-MLGs of *C. pseudonaviculata* found in the six a priori designated populations. The MSN was constructed using similarity percentage and the *imsn* function of the *Poppr* package (Kamvar et al. 2014) in R (R Core Team 2016). To assess the contribution of sexual recombination in contemporary populations of *C. pseudonaviculata*, we measured the index of multilocus association (I_A) and its standardized form ($\bar{r}_D$), which accounts for the number of loci sampled (Agapow and Burt 2001). The null hypothesis of no linkage among markers (panmixia) was tested using 999 bootstrap permutations at $\alpha = 0.05$. Calculations were done using the *Poppr* package (Kamvar et al. 2014) in the R environment (R Core Team 2016).

LeBlanc et al. (2019) described *C. pseudonaviculata* populations present in the United States before 2013 as clonal and with a population structure consistent with asexual reproduction. With these characteristics, *C. pseudonaviculata* populations cannot be examined with Bayesian clustering algorithms such as those implemented in STRUCTURE because these analyses assume Hardy-Weinberg equilibrium and panmixia (Jombart et al. 2010; Pritchard et al. 2000). The genetic structure of the contemporary U.S. population of *C. pseudonaviculata* was analyzed using discriminant analysis of principal components (DAPC), a multivariate, model-free approach that is not founded on assumptions about recombination or unlinked alleles (Jombart et al. 2010). DAPC was performed following the procedure described by Jombart and Collins (2015), using the S*napclust* function implemented in the *Adegenet* package (Jombart 2008) in R (R Core Team 2016) to calculate the optimal *k* value. However, since the Bayesian information criterion did not converge (Supplementary Fig. S2), $k = 6$ was used, based on a priori defined populations.

TABLE 3. Summary of multilocus genotypes (MLGs) found among U.S. isolates of *Calonectria pseudonaviculata*

	Isolates/SSR-MLG[a]				
Population	G1	G2	G9	New	n[b]
East2014	0	34	0	1	35
East2017	0	22	0	0	22
East2018	3	39	0	6	48
East2019	0	36	0	1	37
West2017	2	4	0	1	7
West2019	6	56	4	3	69
Total	11	191	4	12	218

[a] Number of isolates that presented each MLG identified by 11 simple sequence repeat (SSR) markers (SSR-MLG). The SSR-MLGs G1, G2, and G9 described here are the same as those in LeBlanc et al. (2019). New: SSR-MLGs G15 to G24, corresponding to new genotypes identified in this work.
[b] n = total number of isolates.

TABLE 4. Measurement of genetic and genotypic diversity, and linkage disequilibrium for populations of *Calonectria pseudonaviculata* from the United States[a]

Population[b]	n[c]	SSR-MLG[d]	eSSR-MLG[e]	Clonal fraction[f]	SE[g]	H[h]	G[i]	Evenness[j]	H_{exp}[k]
East2014	35	2	1.290	0.943	0.452	0.130	1.06	0.424	0.005
East2017	22	1	1.000	0.955	0.000	0.000	1.00	NaN[l]	0.000
East2018	48	7	2.720	0.854	0.991	0.797	1.50	0.409	0.037
East2019	37	2	1.270	0.946	0.444	0.124	1.06	0.420	0.005
West2017	7	3	3.000	0.571	0.000	0.956	2.33	0.833	0.069
West2019	69	5	2.510	0.928	0.848	0.711	1.49	0.474	0.033
Total	218	13	2.130	0.940	0.901	0.624	1.30	0.343	0.023

[a] Except for the analyses of genotypic diversity, all analyses used clone-corrected datasets.
[b] Populations determined a priori based on sampling year and geographic origin of the samples.
[c] n, number of individuals in each population.
[d] SSR-MLG, number of multilocus genotypes identified with 11 simple sequence repeat (SSR) markers (SSR-MLG).
[e] eSSR-MLG, the number of expected SSR-MLG at the smallest sample size ≥10 based on rarefaction.
[f] Clonal fraction, the proportion of fungal isolates originating from asexual reproduction, calculated as: 1 – [(number of different genotypes)/(total number of isolates)].
[g] SE, standard error based on eSSR-MLG calculations.
[h] H, Shannon-Wiener index of MLG diversity.
[i] G, Stoddart and Taylor's index of MLG diversity.
[j] Evenness, the ratio between the effective number of genotypes and the number of genotypes.
[k] H_{exp}, expected heterozygosity, Nei's genetic diversity index.
[l] NaN, values not calculated due to small sample size.

The distribution of gene diversity and degree of genetic differentiation among populations of *C. pseudonaviculata* were assessed using analysis of molecular variance (AMOVA). We tested the null hypothesis of no differentiation (i) among the six a priori defined populations, (ii) between populations grouped by geographic origin (West versus East U.S. regions), (iii) among populations grouped by year of collection, and (iv) in pairwise comparison between pairs of the six a priori defined populations. Sum of squared size differences were used as the distance measure between two haplotypes (Slatkin 1995). The distributions of the fixation indices were tested using 1,023 permutations by a nonparametric approach (Excoffier et al. 1992) at $\alpha = 0.05$. AMOVAs were carried out using GENODIVE v. 3.03 (Meirmans and Van Tienderen 2004).

Genetic diversity between contemporary populations of *C. pseudonaviculata* from the United States and populations of *C. pseudonaviculata* prior to 2013 from the United States and Europe. DAPC and AMOVA analyses described above were used to test the hypothesis of no genetic differentiation between U.S. *C. pseudonaviculata* populations collected during 2014 to 2019 and the *C. pseudonaviculata* populations recovered from years previous to 2014 from the United States and Europe. In addition, an MSN was constructed as described above to analyze the genetic relationship among the SSR-MLGs of *C. pseudonaviculata* found in the United States and Europe. To conduct these analyses, we retrieved the dataset containing the SSR characterization of 14 *C. pseudonaviculata* isolates from the United States and 60 *C. pseudonaviculata* isolates from Europe previously characterized by LeBlanc et al. (2019). The tests were conducted with clone-corrected data.

RESULTS

A complete SSR dataset was obtained from the 218 *C. pseudonaviculata* isolates, without missing data. From the 11 SSR markers, two markers were monomorphic and eight presented only two alleles (Table 2, Supplementary Table S1). The genotype accumulation curve (Supplementary Fig. S1) showed that the 11 markers identified 92% of the possible genotypes that might exist in the isolate collection. Sequences of the SSR loci were examined for the presence of nucleotide polymorphism within the repetitive motif regions. No homoplasy was detected among isolates with the same genotype for any of the 11 SSR loci (data not shown).

Thirteen SSR-MLGs (SSR-MLGs G1, G2, G9, and G15 to G24) were identified among the 218 isolates (Table 3, Fig. 1). All isolates showed alleles characteristic of *C. pseudonaviculata*, indicating that the sister-species *C. henricotiae* was not present in the U.S. sample examined in this study as of the most recent sampling date (November 2019). Among the genotypes, SSR-MLG G2 was sampled at the highest frequency (88% of the isolates), followed by SSR-MLG G1 (5% of the isolates). Isolates of *C. pseudonaviculata* from sweetbox and pachysandra also belonged to the genotype SSR-MLG G2. The frequency of genotypes SSR-MLGs G9 and G15 to G24 ranged from 0.04 to 1.8% and were represented by one to four isolates each. None of the low frequency genotypes were shared between samples from different states. The genotypes differed at only one locus, and by one or two units of the repetitive motif relative to SSR-MLG G2. The exception was SSR-MLG G16, which differed from SSR-MLG G2 in two loci (SSRs 368 and 1281). The genetic similarity among all SSR-MLGs and their frequency are displayed as an MSN in Figure 1.

Summary statistics calculated for the six populations of *C. pseudonaviculata* defined a priori are summarized in Table 4. The number of genotypes inferred in the populations ranged from one in East2017 to seven in East2018, whereas the clonal fraction ranged from 58% in West2017 to 96% in East2017. The SSR-MLGs were not uniformly distributed, with evenness values as low as 0.41 in East2018 and as high as 0.83 in West2017. Overall, genotypic diversity was low; East2017 was the population with the lowest genotypic diversity (eSSR-MLG = 1, $H_{exp} = 0.00$, and G = 1.0) and West2017 had the highest (eSSR-MLG = 3, $H_{exp} = 0.07$, and G = 2.3).

All 218 *C. pseudonaviculata* isolates amplified the 452-bp fragment characteristic for the idiomorph *MAT1-2* of the mating-type locus (Supplementary Table S1). Both indices of multilocus genetic equilibrium I_A and $\bar{r}_D$ were not significantly different from zero ($P = 0.013$ for East2018, and $P < 0.001$ for the remaining five populations) (Table 5). These results rejected the null hypothesis of panmixia, indicating that *C. pseudonaviculata* populations in the United States reproduce asexually in the area sampled.

DAPC showed an absence of population structure among the six populations of *C. pseudonaviculata* defined a priori, reflecting $k = 1$ (Fig. 2). AMOVA (Supplementary Tables S2 and S3) showed no genetic differentiation among populations when the following structures were tested: (i) populations defined by year and geographic origin ($R_{ST} = 0.19$, $P = 0.962$); (ii) populations grouped according to sampling year, regardless of geographic origin ($R_{CT} = 0.12$, $P = 0.298$); (iii) population samples within the same year ($R_{SC} = 0.34$, $P = 0.904$); (iv) pairwise-comparisons among the six

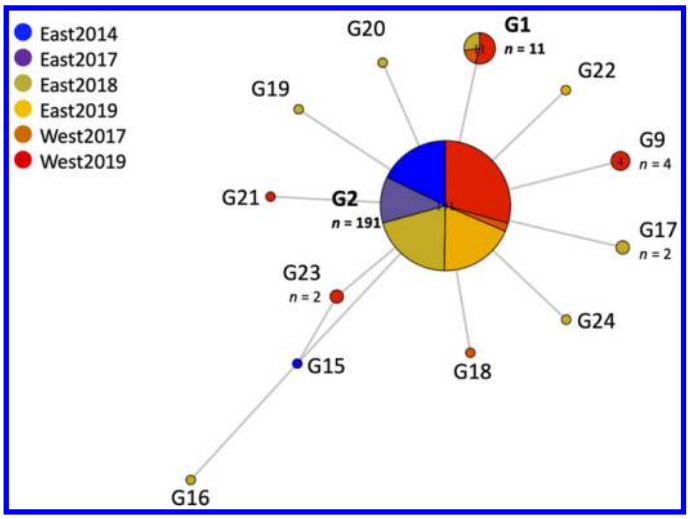

Fig. 1. Minimum spanning network showing the genetic relationship among simple sequence repeat-multilocus genotypes (SSR-MLGs) of 218 isolates of *Calonectria pseudonaviculata* collected in the United States between 2014 and 2019. Isolates were assigned a priori to six populations based on location and year of sampling. Different populations are indicated with different colors. The size of each circle is proportional to the number of isolates in each SSR-MLG; unless otherwise specified, MLGs consist of one *C. pseudonaviculata* isolate.

TABLE 5. Measurement of linkage disequilibrium for populations of *Calonectria pseudonaviculata* from the United States[a]

Population[b]	I_A[c]	I_A P[c,d]	$\bar{r}_D$[e]	$\bar{r}_D$ P[d,e]
East2014	NaN[f]	–	NaN	–
East2017	NaN	–	NaN	–
East2018	–0.667	0.013	–0.111	0.013
East2019	NaN	–	NaN	–
West2017	–0.500	<0.001	–0.500	<0.001
West2019	–0.750	<0.001	–0.250	<0.001
Total	–0.822	<0.001	–0.093	<0.001

[a] Except for the analyses of genotypic diversity, all analyses used clone-corrected datasets.
[b] Populations determined a priori based on sampling year and geographic origin of the samples.
[c] I_A, index of multilocus genetic disequilibrium and its statistical significance.
[d] P, significant departure from the null model of no linkage among markers (panmixia), tested using 999 bootstrap permutations at $\alpha = 0.05$.
[e] $\bar{r}_D$, index of multilocus genetic disequilibrium independent of the number of loci and analyzed by standardization of covariances.
[f] NaN, values not calculated due to small sample size.

populations (R_{ST} ranged from –0.11 to 0.00, all $P \sim 1.00$); and (v) populations grouped within either West or East regions independent of sampling year ($R_{CS} = 0.32$, $P = 0.988$). In contrast, DAPC and AMOVA showed significant genetic differentiation between the West and East sampling regions when the populations were grouped according to sampling location across the years, although the percentage of variation was low ($R_{CT} = 0.14$, $P = 0.012$).

DAPC and AMOVA revealed that contemporary U.S. population of *C. pseudonaviculata* and the population present during the initial introduction and expansion of the disease (2011 to 2013) grouped together into a single cluster ($k = 1$; Supplementary Table S2, Figs. 3 and 4) and were not significantly differentiated ($R_{ST} = 0.002$, $P = 0.425$). On the other hand, the populations from the United States and Europe formed two separate clusters ($k = 2$) and were significantly differentiated into two clonal lineages ($R_{ST} = 0.289$, $P = 0.001$; Fig. 3).

DISCUSSION

Epidemics caused by introduced fungal pathogens typically involve large founder effects meaning that the invasion event is caused by a single or few pathogen genotypes (Drenth et al. 2019).

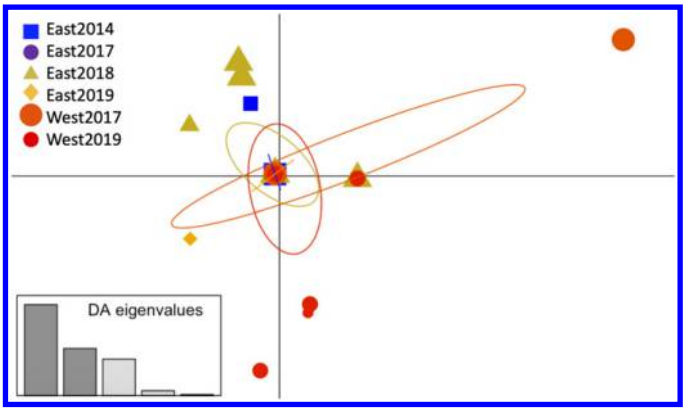

Fig. 2. Scatterplot from discriminant analysis of principal components (DAPC) of six populations of *Calonectria pseudonaviculata* from the United States assigned a priori according to location and year of sampling. The analysis was conducted using clone-corrected data, and each point represents a multilocus genotype. Different populations are indicated with different colors. The ellipses represent the maximum area spanned by 95% of the data in a population.

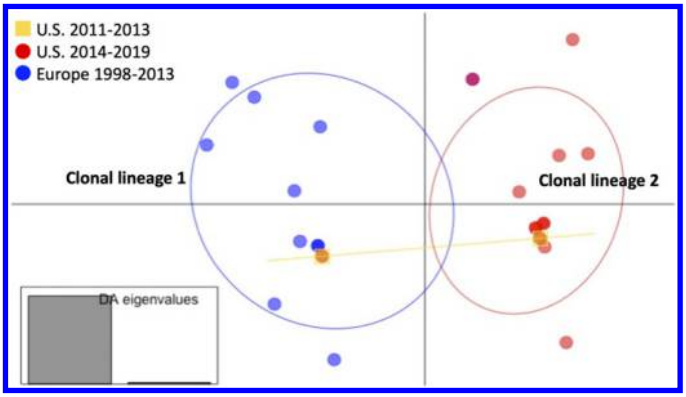

Fig. 3. Scatterplot from discriminant analysis of principal components (DAPC) of populations of *Calonectria pseudonaviculata* from the United States and Europe assigned a priori according to location and year of sampling. The analysis was conducted using clone-corrected data, and each point represents a multilocus genotype. Different populations are indicated with different colors. The ellipses represent the maximum area spanned by 95% of the data in a population.

Even though nine years have passed since the first U.S. outbreaks of boxwood blight, the contemporary *C. pseudonaviculata* population still exhibits the distinctive features of an introduced species, including a clonal population structure, predominance of a few MLGs at high frequencies over a wide geographic area and repeatedly recovered across several years, no subdivision among subpopulations, exclusive presence of one mating type, and no evidence of sexual recombination in the invaded area (Gladieux et al. 2015). These population characteristics are the hallmarks of numerous invasive plant pathogens, including some of the most damaging fungal and oomycete plant pathogens introduced to the United States, including *Ophiostoma novo-ulmi* (Dutch elm disease; Brasier 2001), *Cryphonectria parasitica* (chestnut blight; Pautasso 2013), *Raffaelea lauricola* (laurel wilt; Wuest et al. 2017), and *Phytophthora ramorum* (sudden oak death; Kamvar et al. 2015).

The U.S. populations of *C. pseudonaviculata* before and after 2014 are not differentiated, indicating that the overall genetic composition of the pathogen population has not markedly changed since the first U.S. disease outbreaks in 2011. Moreover, SSR-MLG G1 and G2 are the only two genotypes found in populations from the United States prior to and post 2014 at similar frequencies. SSR-MLG G2 and G1 represented 88 and 5% of the isolates of the contemporary population of *C. pseudonaviculata*, respectively. Likewise, in the U.S. population prior to 2013, SSR-MLG G2 was represented by 93% of the isolates and SSR-MLG G1 by 7% (LeBlanc et al. 2019). SSR-MLG G2 has also been found in Europe, and G1 was detected in Europe, Asia and New Zealand (LeBlanc et al. 2019). This suggests that the genotypes that founded the *C. pseudonaviculata* population in the United States may themselves have originated from established disease centers in Asia, Europe, or New Zealand, but we cannot exclude the possible involvement of another unknown source(s).

A third genotype, SSR-MLG G9, was detected from four different cultivars of *B. sempervirens* found in two blocks in a commercial nursery in OR in 2019. This genotype was previously identified in samples from the United Kingdom in 2012, but this is the first report of this genotype in the United States. The presence of SSR-MLG G9 in the United States could be the result of either an introduction from Europe, or a random somatic mutation in resident *C. pseudonaviculata* populations that resulted in the convergent

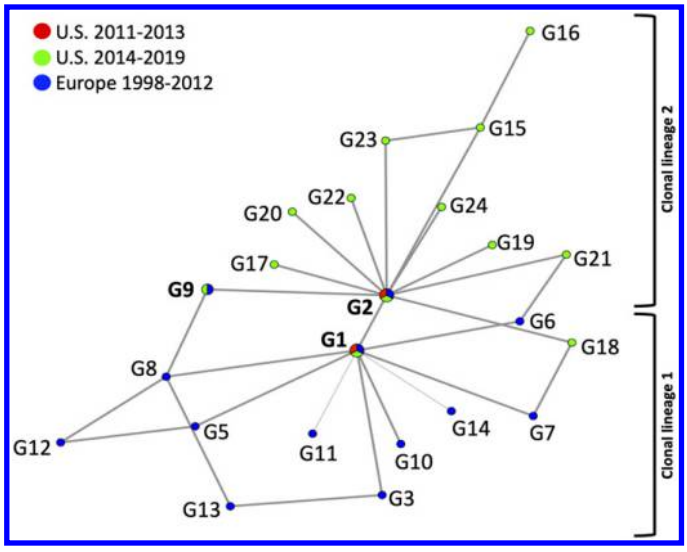

Fig. 4. Minimum spanning network showing the genetic relationship among 24 simple sequence repeat-multilocus genotypes of *Calonectria pseudonaviculata* collected in the United States and Europe between 1998 and 2019. The analysis was conducted using clone-corrected data. Different populations are indicated with different colors.

evolution of an MLG identical to that found in Europe. Although the overall homogeneity of *C. pseudonaviculata* populations in general argues against the second option, convergent evolution may be a plausible explanation considering the limited genetic difference between SSR-MLG G9 and G1 (one unit of the repetitive motif in the SSR 1281).

Ten additional *C. pseudonaviculata* MLGs (SSR-MLGs G15 to G24) were found in low frequency and constitute new genotypes found only in the United States after 2014. All of the new genotypes except SSR-MLG G16 differ from SSR-MLG G2 by one SSR locus and by one unit of the repetitive motif. Similarly, the minor genetic difference between SSR-MLG G2 and the new genotypes shown by the MSN and DAPC suggest that they most likely originated by accumulation of random somatic mutations (Taylor et al. 2015). Interestingly, the 10 new SSR-MLGs have each only been recovered from single locations and sampling years. The reasons for this could be numerous. It is possible that the new genotypes were not detected in other locations due to bias in fungal isolation technique and sampling structure. In addition, these hypothetical unsampled genotypes might not be fit enough to persist through time; their disease ecology might not allow involve survival as asymptomatic endophytes or in latent infections. Future studies that deploy the use of stratified sampling from symptomatic and asymptomatic plants may result in answers to these questions.

Our results suggest that *C. pseudonaviculata* populations from the United States and Europe are significantly differentiated. The global population structure of numerous invasive plant pathogens, namely *Verticillium dahliae*, *Puccinia striiformis*, and *Phytophthora* spp., are characterized by strong differentiation among populations that are geographically separated (Ali et al. 2014; McDonald and Stukenbrock 2016). Several processes can serve to separate geographically disconnected populations. In pathogens that have been moved to a new region, individuals with novel traits can emerge and spread without completely replacing the existing ones. This may be occurring in the United States as new *C. pseudonaviculata* genotypes evolve in place, as observed with the emergence of SSR-MLGs G15 to G24. In addition, gene flow between the source and newly established populations might not be possible due to geographical barriers (oceans, mountains, etc.) or anthropogenic activities (trade regulations and quarantines). This contributes to the genetic differentiation among geographically isolated populations being maintained and increasing over time (McDonald and Stukenbrock 2016). Stringent trade regulations that limit movement of foreign boxwood plants into the United States were only recently adopted by USDA-APHIS in March 2020 (https://www.perishablenews.com/floral/aphis-amends-entry-requirements-for-importation-of-boxwood-euonymus-and-holly-from-canada-into-the-united-states/). Although the importation regulations were implemented to keep the box tree moth (*Cydalima perspectalis*) from entering the United States, these new restrictions will likely also reduce any further movement of *C. pseudonaviculata* from foreign sources, suggesting that the observed differentiation between global *C. pseudonaviculata* populations will likely increase.

At this point it is important to remark that the SSR genetic markers used in this research are useful for identifying population structure and diversity, but they cannot identify genes in underlying correlated phenotypes in the clonal population. The association between clonal lineages and phenotypic races or virulence spectra range from perfect, like *Fusarium oxysporum*, to nonexistent, such as in populations of *Phytophthora infestans* (Milgroom 2017). At present, there is no data about the presence of races or differences in the pathogenic spectra of individual isolates of *C. pseudonaviculata.* Studies documenting pathogenic diversity and aggressiveness among isolates of *C. pseudonaviculata* have given contradictory results (Daughtrey 2019). Gehesquière et al. (2016) and LaMondia and Shishkoff (2017) did not observe differences in virulence/aggressiveness among isolates of *C. pseudonaviculata* and *C. henricotiae*. On the other hand, Khazaeli et al. (2018) reported significant differences in the virulence level of *C. pseudonaviculata* isolates from Iran in inoculation tests on *B. sempervirens* subsp. *hyrcana*. These inconsistencies may be compared with differences in the isolates used for disease evaluation in Iran, relative to those studied by U.S. and European scientists. Unlike the United States and Europe, where *C. pseudonaviculata* isolates all possess SSR-MLGs that fall within CL1 and CL2, some *C. pseudonaviculata* isolates in Iran have been shown to belong to a different genotype, SSR-MLG G4 (LeBlanc et al. 2019). Nonetheless, we cannot assume that isolates sharing the same MLG will show the same pathogenicity/virulence toward different host species and cultivars (Taylor et al. 2017). Phenotypic analysis for studying the pathogenic/virulence diversity present in the contemporary population of *C. pseudonaviculata* in the United States, especially investigating the new SSR-MLGs, will be important for the breeding of durable resistant germplasm and cultivars.

The invasion of new environments exerts a continuous pressure on pathogen populations to adapt to conditions that are distinct from those in their native range (Gladieux et al. 2015). Responding to this selective pressure and/or the chance to encounter a novel host that does not have coevolved resistance commonly leads to host-shifts, host-jumps, host-range expansions, or changes in aggressiveness, especially when the newly invaded environment is connected to the agricultural practice of growing very dense, homogeneous populations of host plants on vast spatial and temporal scales (Gladieux et al. 2015; Henricot et al. 2017; Hovmøller et al. 2008; McDonald and Stukenbrock 2016). In addition to causing boxwood blight, *C. pseudonaviculata* also causes foliar blight diseases of sweetbox (Kong et al. 2017a; Ryan et al. 2018) and pachysandra (Kong et al. 2017a; LaMondia et al. 2012), plants that also belong to the family *Buxaceae. C. pseudonaviculata* was shown to be also capable of infecting other boxwood companion plants outside the family *Buxaceae* in artificial inoculations (Richardson et al. 2020). In our study and in previous work (LeBlanc et al. 2019), four isolates of *C. pseudonaviculata* recovered from pachysandra and sweetbox were genotyped as members of the predominant SSR-MLG G2 and did not show any genetic difference that might be evidenced with SSR markers, with respect to other isolates of the same MLG recovered from boxwood plants. Together these findings show that individuals in the *C. pseudonaviculata* SSR-MLG G2 (CL2) can expand their host range, either in response to adaptive pressure and/or chance of facing a new susceptible host. Being aware of this capability for host range expansion is critical and should be considered when developing and implementing disease management programs (Daughtrey 2019; Stukenbrock and McDonald 2008).

Another commonly observed trait of introduced plant pathogens is the loss of sexual reproduction (Gladieux et al. 2015). The presence of only one mating-type idiomorph (*MAT1-2*) and linkage disequilibrium indicates that asexual reproduction predominates throughout the known range of *C. pseudonaviculata* (this study; Gehesquière et al. 2016; LeBlanc et al. 2019). However, rapid significant evolutionary changes are possible even in the absence of sexual recombination (Croll 2016). Furthermore, the absence of signal for recombination should not be interpreted as a lack of sex in the species (Drenth et al. 2019). Several fungi have been reported to sexually reproduce in their center of origin and/or more heterogenous host populations in the wild (Gladieux et al. 2015; Saleh et al. 2012). The center of origin for *C. pseudonaviculata* is undetermined, but may lie within the natural range of the genus *Buxus* in one of the host centers of diversity: East Asia, the Caribbean, or Madagascar (Köhler 2004).

Diversity in clonal populations is well explained in terms of clonal evolutionary genetic lineages rather than as individual MLGs (Arnaud-Haond et al. 2008; Milgroom 2017; Taylor et al. 2015). Anderson and Kohn (1995) defined clonal lineages as "the asexual descendants of a given genotype differing from the originator only via mutation and mitotic recombination." This means that all isolates showing identical MLGs originated from the same organism through

asexual reproduction, composing a homogeneous clonal lineage that contains highly similar, but not identical, clonal genotypes. As a result, clonal lineages can be relatively diverse, due to the accumulation of mutations over the course of successive cycles of asexual reproduction (Anderson and Kohn 1995; Milgroom 2017). Considering the clonal nature of populations of the boxwood blight pathogen evidenced by our findings and supported by previous studies (LeBlanc et al. 2019; Malapi-Wight et al. 2019), it seems appropriate to adopt the concept of clonal lineage. Therefore, we consider the *C. pseudonaviculata* population to be composed of two clonal lineages, namely CL1, which is a homogenous lineage made up of SSR-MLG G1 and G9, and CL2, a more diverse lineage containing SSR-MLG G2 and the 10 new genotypes, all of which are unlikely to have arisen independently through sexual reproduction. Both CL1 and CL2 have been found since the beginning of the boxwood blight epidemic in the United States; however, CL2 is the more prevalent and widespread lineage. CL2 was the clonal lineage identified in the new disease occurrences during 2018 and 2019: the first *C. pseudonaviculata* isolates recovered from the states of AR, GA, IN, KY, OH, SC, TN, and WI all belong to SSR-MLG G2. Together, these data indicate that CL2 is at the expanding front of the U.S. boxwood blight epidemic.

The use of SSR markers to genotype a very genetically uniform, asexual population such as the contemporary population of *C. pseudonaviculata* in the United States has some drawbacks. As shown by the genotype accumulation curve (Supplementary Fig. S1), the 11 SSR markers were predicted to resolve <100% of the potential diversity present in the isolate collection. Secondly, analyses of historical or contemporary directional migrations are not possible (Grünwald et al. 2016; Milgroom 2017). Population genomics studies using whole-genome GBS approach are ongoing in our research group (N. LeBlanc and J. A. Crouch, *personal communication*). These studies will expand our understanding of the temporal and spatial evolution of the boxwood blight epidemic.

ACKNOWLEDGMENTS

We thank the numerous individuals responsible for documenting boxwood blight and sharing disease samples.

LITERATURE CITED

Agapow, P. M., and Burt, A. 2001. Indices of multilocus linkage disequilibrium. Mol. Ecol. Notes 1:101-102.

Ali, S., Gladieux, P., Leconte, M., Gautier, A., Justesen, A. F., Hovmøller, M. S., Enjalbert, J., and de Vallavieille-Pope, C. 2014. Origin, migration routes and worldwide population genetic structure of the wheat yellow rust pathogen *Puccinia striiformis* f. sp. *tritici*. PLoS Pathog 10:e1003903.

Anderson, J. B., and Kohn, L. M. 1995. Clonality in soilborne plant pathogenic fungi. Annu. Rev. Phytopathol. 33:369-391.

Arnaud-Haond, S., Duarte, C., Filipe, A., and Serrao, E. 2008. Standardizing methods to address clonality in population studies. Mol. Ecol. 16: 5115-5139.

Beirn, L. A., Hempfling, J. W., Schmid, C. J., Murphy, J. A., Clarke, B. B., and Crouch, J. A. 2017. Differences among soil-inhabiting microbial communities in *Poa annua* turf throughout the growing season. Crop Sci.: S262-S273.

Brasier, C. M. 2001. Rapid evolution of introduced plant pathogens via interspecific hybridization: hybridization is leading to rapid evolution of Dutch elm disease and other fungal plant pathogens. Bioscience 51: 123-133.

Castroagudín, V. L., Yang, X., Daughtrey, M. L., Luster, D. G., Pscheidt, J. W., Weiland, J. E., and Crouch, J. A. 2020. Boxwood blight disease: A diagnostic guide. Plant Health Prog. https://doi.org/10.1094/PHP-06-20-0053-DG

Croll, D. 2016. Evolution in the absence of sex: Ideas revisited in the post-genomics age. BioEssays 38:1191.

Crous, P. W., Groenewald, J. Z., and Hill, C. F. 2002. *Cylindrocladium pseudonaviculatum* sp. nov. from New Zealand, and new *Cylindrocladium* records from Vietnam. Sydowia 54:23-33.

Daughtrey, M. L. 2019. Boxwood blight: Threat to ornamentals. Annu. Rev. Phytopathol. 57:189-209.

Decocq, G., Bordier, D., Wattez, J. R., and Racinet, P. 2014. A practical approach to assess the native status of a rare plant species: The controverse of *Buxus sempervirens* L. in northern France revisited. Plant Ecol. 173: 139-151.

Drenth, A., McTaggart, A. R., and Wingfield, B. D. 2019. Fungal clones win the battle, but recombination wins the war. IMA Fungus 10:18.

Elmhirst, J. F., Auxier, B. E., and Wegener, L. A. 2013. First report of box blight caused by *Cylindrocladium pseudonaviculatum* (*C. buxicola*) in British Columbia, Canada. Plant Dis. 97:559.

Excoffier, L., Smouse, P. E., and Quattro, J. M. 1992. Analysis of molecular variance inferred from metric distances among DNA haplotypes: Application to human mitochondrial DNA restriction data. Genetics 131:479-491.

Fox, E. J., Reid-Bayliss, K. S., Emond, M. J., and Loeb, L. A. 2014. Accuracy of next generation sequencing platforms. Next Gener. Seq. Appl. 1: 1000106.

Gehesquière, B., Crouch, J. A., Marra, R. E., Van Poucke, K., Rys, F., Maes, M., Gobin, B., Höfte, M., and Heungens, K. 2016. Characterization and taxonomic reassessment of the box blight pathogen *Calonectria pseudonaviculata*, introducing *Calonectria henricotiae* sp. nov. Plant Pathol. 65: 37-52.

Gladieux, P., Feurtey, A., Hood, M. E., Snirc, A., Clavel, J., Dutech, C., Roy, M., and Giraud, T. 2015. The population biology of fungal invasions. Mol. Ecol. Notes 24:1969-1986.

Grünwald, N. J., McDonald, B. A., and Milgroom, M. G. 2016. Population genomics of fungal and oomycete pathogens. Annu. Rev. Phytopathol. 54: 323-346.

Henricot, B., and Culham, A. 2002. *Cylindrocladium buxicola*, a new species affecting *Buxus* spp., and its phylogenetic status. Mycologia 94:980-997.

Henricot, B., Pérez-Sierra, A., Armstrong, A. C., Sharp, P. M., and Green, S. 2017. Morphological and genetic analyses of the invasive forest pathogen *Phytophthora austrocedri* reveal that two clonal lineages colonized Britain and Argentina from a common ancestral population. Phytopathology 107: 1532-1540.

Henricot, B., Pérez Sierra, A., and Prior, C. 2000. A new blight disease on *Buxus* in the UK caused by the fungus *Cylindrocladium*. Plant Pathol. 49: 805.

Hovmøller, M. S., Yahyaoui, A. H., Milus, E. A., and Justesen, A. F. 2008. Rapid global spread of two aggressive strains of a wheat rust fungus. Mol. Ecol. 17:3818-3826.

Ivors, K. L., Lacey, L. W., Milks, D. C., Douglas, S. M., Inman, M. K., Marra, R. E., and LaMondia, J. A. 2012. First report of boxwood blight caused by *Cylindrocladium pseudonaviculatum* in the United States. Plant Dis. 96: 1070.

Jombart, T. 2008. Adegenet: A R package for the multivariate analysis of genetic markers. Bioinformatics 24:1403-1405.

Jombart, T., and Collins, C. 2015. A tutorial for discriminant analysis of principal components (DAPC) using adegenet 2.0.0. https://adegenet.r-forge.r-project.org/files/tutorial-dapc.pdf

Jombart, T., Devillard, S., and Balloux, F. 2010. Discriminant analysis of principal components: A new method for the analysis of genetically structured populations. BMC Genet. 11:94.

Kamvar, Z. N., Larsen, M. M., Kanaskie, A. M., Hansen, E. M., and Grünwald, N. J. 2015. Spatial and temporal analysis of populations of the sudden oak death pathogen in Oregon forests. Phytopathology 105:982-989.

Kamvar, Z. N., Tabima, J. F., and Grunwald, N. 2014. Poppr: An R package for genetic analysis of populations with clonal, partially clonal, and/or sexual reproduction. PeerJ 2:e281.

Khazaeli, P., Rezaee, S., Mirabolfathy, M., Zamanizadeh, H., and Kiadaliri, H. 2018. Genetic and phenotypic variation of *Calonectria pseudonaviculata* isolates causing boxwood blight disease in the Hyrcanian forest of Iran. Agri. Res. & Tech.: Open Access J 19:ARTOAJ.MS.ID.19.556081.

Köhler, E. 2004. The genus *Buxus* (*Buxaceae*). Rev. Jard. Bot. Nac. Univ. Habana 25/26:17-23.

Kong, P., Likins, T. M., and Hong, C. X. 2017a. First report of *Pachysandra terminalis* leaf spot by *Calonectria pseudonaviculata* in Virginia. Plant Dis. 101:509.

Kong, P., Likins, T. M., and Hong, C. X. 2017b. First report of blight of *Sarcococca hookeriana* var. *humilis* by *Calonectria pseudonaviculata* in Virginia. Plant Dis. 101:247.

LaMondia, J. A., Li, D. W., Marra, R. E., and Douglas, S. M. 2012. First report of *Cylindrocladium pseudonaviculatum* causing leaf spot of *Pachysandra terminalis*. Plant Dis. 96:1069.

LaMondia, J. A., and Shishkoff, N. 2017. Susceptibility of boxwood accessions from the national boxwood collection to boxwood blight and potential for differences between *Calonectria pseudonaviculata* and *C. henricotiae*. HortScience 52:873-879.

LeBlanc, N., and Crouch, J. A. 2019. Prokaryotic taxa play keystone roles in the soil microbiome associated with woody perennial plants in the genus *Buxus*. Ecol. Evol. 9:11102-11111.

LeBlanc, N., Gehesquière, B., Salgado-Salazar, C., Heungens, K., and Crouch, J. A. 2019. Limited genetic diversity across pathogen populations responsible for the global emergence of boxwood blight identified using SSRs. Plant Pathol. 68:861-868.

LeBlanc, N. L., Salgado-Salazar, C., and Crouch, J. A. 2018. Boxwood blight: An ongoing threat to ornamental and native boxwood. Appl. Microbiol. Biotechnol. 102:4371-4380.

Ma, X., Shao, Y., Tian, L., Flasch, D. A., et al. 2019. Analysis of error profiles in deep next-generation sequencing data. Genome Biol. 20:50.

Malapi-Wight, M., Salgado-Salazar, C., Demers, J. E., Clement, D. L., Rane, K. K., and Crouch, J. A. 2016. Sarcococca blight: Use of whole-genome sequencing for fungal plant disease diagnosis. Plant Dis. 100:1093-1100.

Malapi-Wight, M., Veltri, D., Gehesquière, B., Heungens, K., Rivera, Y., Salgado-Salazar, C., and Crouch, J. A. 2019. Global distribution of mating types shows limited opportunities for mating across populations of fungi causing boxwood blight disease. Fungal Genet. Biol. 131:103246.

McDonald, B. A., and Stukenbrock, E. H. 2016. Rapid emergence of pathogens in agro-ecosystems: Global threats to agricultural sustainability and food security. Philos. Trans. R. Soc. B 371:20160026.

Meirmans, P. G., and Van Tienderen, P. H. 2004. GENOTYPE and GENODIVE: Two programs for the analysis of genetic diversity of asexual organisms. Mol. Ecol. Notes 4:792-794.

Milgroom, M. G. 2017. Population Biology of Plant Pathogens: Genetics, Ecology and Evolution. American Phytopathology Society, St. Paul, MN.

Miller, M. E., Shishkoff, N., and Cubeta, M. A. 2018. Thermal sensitivity of *Calonectria henricotiae* and *Calonectria pseudonaviculata* conidia and microsclerotia. Mycologia 110:546-558.

Mitchell, R., Chitanava, S., Dbar, R., Kramarets, V., Lehtijärvi, A., Matchutadze, I., Mamadashvili, G., Matsiakh, I., Nacambo, S., Papazova-Anakieva, I., Sathyapala, S., Tuniyev, B., Vétek, G., Zukhbaia, M., and Kenis, M. 2018. Identifying the ecological and societal consequences of a decline in *Buxus* forests in Europe and the Caucasus. Biol. Invasions 20:3605-3620.

Pautasso, M. 2013. Responding to diseases caused by exotic tree pathogens. Pages 592-612 in: Infectious Forest Diseases. P. Gonthier and G. Nicolotti, eds. CABI, Wallingford, U.K.

Pritchard, J. K., Stephens, M., and Donnelly, P. 2000. Inference of population structure using multilocus genotype data. Genetics 155:945-959.

R Core Team. 2016. R: A Language and Environment for Statistical Computing. R Foundation for Statistical Computing, Vienna, Austria. http://www.R-project.org/

Richardson, P. A., Daughtrey, M., and Hong, C. X. 2020. Indications of susceptibility to *Calonectria pseudonaviculata* in some common groundcovers and boxwood companion plants. Plant Dis. 104:1127-1132.

Ryan, C., Williams-Woodward, J., and Zhang, D. L. 2018. Susceptibility of *Sarcococca* taxa to boxwood blight by *Calonectria pseudonaviculata.* Pages 64-67 in: Proceedings of Southern Nursery Association Research Conference, Vol. 62.

Sacher, G. O., Weiland, D. E., Putnam, M. L., Crouch, J. A., and Castroagudín, V. L. 2020. Confirmation of *Calonectria pseudonaviculata* causing boxwood blight of *Buxus* cultivars in Oregon. Plant Dis. 104:1862.

Saleh, D., Xu, P., Shen, Y., Li, C., Adreit, H., Milazzo, J., Ravigne, V., Bazin, E., Nottéghem, J. L., Fournier, E., and Tharreau, D. 2012. Sex at the origin: An Asian population of the rice blast fungus *Magnaporthe oryzae* reproduces sexually. Mol. Ecol. 21:1330-1344.

Salgado-Salazar, C., Shishkoff, N., LeBlanc, N., Ismaiel, A. A., Collins, M., Cubeta, M. A., and Crouch, J. A. 2019. *Coccinonectria pachysandricola*, causal agent of a new foliar blight disease of *Sarcococca hookeriana*. Plant Dis. 103:1337-1346.

Šarhanová, P., Pfanzelt, S., Brandt, R., Himmelbach, A., and Blattner, F. R. 2018. SSR-seq: Genotyping of microsatellites using next-generation sequencing reveals higher level of polymorphism as compared to traditional fragment size scoring. Ecol. Evol. 8:10817-10833.

Shishkoff, N. 2016. Survival of microsclerotia of *Calonectria pseudonaviculata* and *C. henricotiae* exposed to sanitizers. Plant Health Prog. 17:13-17.

Slatkin, M. 1995. A measure of population subdivision based on microsatellite allele frequencies. Genetics 139:457-462.

Stravoravdis, S., LeBlanc, N. R., Marra, R. E., Crouch, J. A., and Hulvey, J. P. 2020. Widespread occurrence of a CYP51A pseudogene in *Calonectria pseudonaviculata*. Mycobiology 48:44-50.

Stukenbrock, E. H., and McDonald, B. A. 2008. The origins of plant pathogens in agro-ecosystems. Annu. Rev. Phytopathol. 46:75-100.

Taylor, J. W., Branco, S., Gao, C., Hann-Soden, C., Montoya, L., Sylvain, I., and Gladieux, P. 2017. Sources of fungal genetic variation and associating it with phenotypic diversity. Microbiol. Spectr. 5:1-21.

Taylor, J. W., Hann-Soden, C., Branco, S., Sylvain, I., and Ellison, C. E. 2015. Clonal reproduction in fungi. Proc. Natl. Acad. Sci. USA 112:8901-8908.

Tibihika, P. D., Curto, M., Dornstauder-Schrammel, E., Winter, S., Alemayehu, E., Waidbacher, H., and Meimberg, H. 2018. Application of microsatellite genotyping by sequencing (SSR-GBS) to measure genetic diversity of the East African *Oreochromis niloticus*. Conserv. Genet. 20: 357-372.

Tuite, J. 1969. Pathological Methods: Fungi and Bacteria. Burgess Publishing Company, Minneapolis, MN.

Wuest, C. E., Harrington, T. C., Fraedrich, S. W., Yun, H.-Y., and Lu, S.-S. 2017. Genetic variation in native populations of the laurel wilt pathogen, *Raffaelea lauricola*, in Taiwan and Japan and the introduced population in the United States. Plant Dis. 101:619-628.

Zhang, J., Kobert, K., Flouri, T., and Stamatakis, A. 2014. PEAR: A fast and accurate Illumina Paired-End reAd mergeR. Bioinformatics 20: 614-620.